PCCP

PAPER

Formation of intra-island grain boundaries in pentacene monolayers

Jian Zhang,[*ab] **Yu Wu,**[c] **Steffen Duhm,**[ad] **Jürgen P. Rabe,**[a] **Petra Rudolf**[*c] **and Norbert Koch**[*a]

To assess the formation of intra-island grain boundaries during the early stages of pentacene film growth, we studied sub-monolayers of pentacene on pristine silicon oxide and silicon oxide with high pinning centre density (induced by UV/O_3 treatment). We investigated the influence of the kinetic energy of the impinging molecules on the sub-monolayer growth by comparing organic molecular beam deposition (OMBD) and supersonic molecular beam deposition (SuMBD). For pentacene films fabricated by OMBD, higher pentacene island-density and higher polycrystalline island density were observed on UV/O_3-treated silicon oxide as compared to pristine silicon oxide. Pentacene films deposited by SuMBD exhibited about one order of magnitude lower island- and polycrystalline island densities compared to OMBD, on both types of substrates. Our results suggest that polycrystalline growth of single islands on amorphous silicon oxide is facilitated by structural/chemical surface pinning centres, which act as nucleation centres for multiple grain formation in a single island. Furthermore, the overall lower intra-island grain boundary density in pentacene films fabricated by SuMBD reduces the number of charge carrier trapping sites specific to grain boundaries and should thus help achieving higher charge carrier mobilities, which are advantageous for their use in organic thin-film transistors.

Introduction

Organic materials have huge potential for use in (opto-) electronic devices, such as organic photovoltaic cells and organic thin-film transistors (OTFTs).[1–8] Among the various molecular materials being studied, pentacene $(C_{22}H_{14})$[1,2,6,7] is a very promising candidate for future devices since a charge carrier mobility at room temperature of up to 35 cm^2 V^{-1} s^{-1} (for holes), a value higher than that of hydrogenated amorphous silicon, has been reported for pentacene single crystals.[9] However, the maximum field-effect mobility in polycrystalline pentacene films is only ~5 cm^2 V^{-1} s^{-1}.[1,2] Therefore, an optimization of pentacene thin film growth is desired in order to minimise the abundance of grain boundaries, since the latter act as bottleneck for fast carrier transport.[1–8] Significant efforts have already been directed towards understanding the growth dynamics of pentacene films.[10–14] Most studies were

focused on the pentacene monolayer at the interface to a prototypical gate dielectric (silicon oxide) in OTFTs because the first molecular layer acts as a template for successive layers, and therefore impacts the morphology and the structure of the film.[12,15] Furthermore, charge transport in OTFTs is confined to the first few molecular layers on the gate insulator, which implies that the molecular monolayer at the interface is of utmost importance for achieving good charge transport properties in devices.[16–19]

Self-driven polycrystallization has been directly observed from a single nucleus in the case of epitaxial pentacene growth on Si(111)-H terminated surfaces under ultrahigh vacuum.[20] The observed polycrystallization is supposed to be a result of kinetic growth parameters in conjunction with the intrinsic anisotropy of the crystal structure, which indicates that polycrystallization might be an intrinsic property of pentacene films. Another study evidenced polycrystallization within single pentacene topographical islands in pentacene (sub)monolayers on amorphous silicon oxide substrates, and reported the grain-boundary evolution as a function of coverage.[21] Since pentacene condensation is controlled by relatively weak van der Waals interactions (between molecules and with silicon oxide), the nucleation process is extremely sensitive to defects or impurities on the substrate surface that can act as pinning sites. To unravel whether the formation of polycrystalline islands on silicon oxide is an intrinsic material property or substrate-mediated by pinning sites, we compared the evolution of intra-island grain boundaries

[a] *Institut für Physik, Humboldt-Universität zu Berlin, Newtonstrasse 15, D-12489 Berlin, Germany. E-mail: norbert.koch@physik.hu-berlin.de*
[b] *State Key Laboratory of Catalysis, Dalian Institute of Chemical Physics, 457 Zhongshan Road, 116023 Dalian, China. E-mail: jianzhang@dicp.ac.cn*
[c] *Zernike Institute for Advanced Materials, University of Groningen, Nijenborgh 4, NL-9747AG Groningen, The Netherlands. E-mail: p.rudolf@rug.nl*
[d] *Graduate School of Advanced Integration Science, Chiba University, 1-33 Yayoi-cho, Chiba 263-8522, Japan*

in the early stages of pentacene growth on pristine (low pinning site density) and UV/O$_3$-treated (high pinning site density) silicon oxide. In addition, we investigated the impact of the kinetic energy of molecules arriving at the substrate surface by comparing standard OMBD and SuMBD.

Materials and methods

Substrate preparation

280 nm thick silicon oxide/silicon wafers (purchased from Silicon Quest International, USA) were used as substrates. These wafers were cleaved into 10×10 mm^2 pieces and cleaned by sonication in acetone for 5 min. Then wafers were transferred into iso-propan-2-ol ((CH$_3$)$_2$CHOH) and sonicated for another 5 min, followed by sonication in deionised water for 5 min and rinsing in deionised water (DI water). Finally they were dried by spinning and blowing with N$_2$ (99.995%) gas.

To obtain substrates with higher density of surface pinning sites, we subsequently applied a 20 min UV/O$_3$ treatment to half of the cleaned wafer pieces, using a low-pressure mercury Pen–Ray lamp (UVP, Inc.) under ambient conditions. The samples were positioned at *ca.* 1 cm below the lamp, and the setup was covered with a glass bowl to increase local O$_3$ concentration. Note that in addition to O$_3$ singlet O$_2$ was also produced, which will not be referred to separately in the following. The surface properties of the pristine and UV/O$_3$ treated silicon oxide were characterised by contact angle measurements (sessile drop method).[22]

Film preparation

Pentacene films by organic molecular beam deposition. Pentacene (99.5%; Aldrich Chemical Co.) was used as received. Pentacene films were evaporated onto pristine and UV/O$_3$-treated silicon oxides in a high vacuum chamber with a pressure during evaporation of 2×10^{-7} mbar. Under these conditions, a monolayer coverage of the surfaces with adsorbed water may persist.[23] The deposition rate was monitored with a quartz crystal microbalance and equal to 0.3–0.5 Å min^{-1}. The substrate was held at room temperature during deposition. Throughout the text, we express film thicknesses by an equivalent amount of standing, close-packed monolayers (1 ML = 15 Å).

Pentacene films by supersonic molecular beam deposition (SuMBD). In SuMBE the molecular species is seeded in a beam of lighter noble gas or H$_2$. A free-jet expansion allows control of the kinetic energy and momentum of the molecules as well as the flux by changing the source parameters.[24] The kinetic energy of the impinging molecules can thus be tuned from less than 1 eV up to several tens of eV, *i.e.*, within a range of energies of surface processes such as elastic-inelastic scattering, physisorption, chemisorption, and activation of surface chemical reactions. Hyperthermal energies reached using supersonic beam methods have given access to controlling growth,[25] reactivity,[26] morphology and structure[27,28] of molecular thin films beyond the level achievable by OMBD.

The SuMBD system is essentially the same as previously described.[14,28] Under our experimental conditions, the kinetic energy of 6.4 eV was achieved by properly varying the degree of seeding through changing the He carrier gas pressure.

Therefore, in SuMBD pentacene molecules diffuse much longer on pristine and UV/O$_3$-treated silicon oxides than in OMBD, where the velocity of the impinging molecules follows a Maxwell Boltzmann distribution, centred around a value which is ~ 20 times smaller than the velocity of the molecules in the supersonic beam. In SuMBD the pentacene molecules also have enough kinetic energy not to be trapped easily at the pinning centres. The substrates were mildly heated (423–473 K) before deposition to desorb physisorbed species, particularly water. However, since no liquid-nitrogen cooled trap was present on the gas line, the presence of residual water in the monolayer range cannot be totally excluded. The samples were prepared by exposing the substrates to the supersonic beam impinging on a surface area of ~ 10 mm diameter. For different exposure times (5 min, 10 min and 15 min), at room temperature, the corresponding coverage of pentacene films is about 0.15 ML, 0.30 ML and 0.45 ML as determined from the analysis of the atomic force microscopy images.

Film characterisation

X-Ray photoelectron spectroscopy (XPS). Substrates obtained after each of the preparation steps outlined above were introduced into the load lock (base pressure: 5×10^{-7} mbar) of the UHV system containing the X-ray photoelectron spectrometer within less than 10 min after preparation for elemental analysis. The UV/O$_3$-treated substrate was introduced into the load lock of the UHV-system directly after UV/O$_3$ treatment and measured approximately 1 h later. XPS spectra were recorded using Al K$_\alpha$ radiation and a hemispherical analyser. The base pressure in the spectrometer was 1.1×10^{-10} mbar. Spectral analysis included a Shirley background subtraction and peak separation using mixed Gaussian–Lorentzian functions in a least squares curve-fitting program (WINSPEC) developed in the LISE laboratory of the University of Namur, Belgium.

Atomic force microscopy (AFM)/transverse shear microscopy (TSM). Pristine and UV/O$_3$-treated silicon oxides were analysed with AFM (Digital Instruments, Nanoscope IV) in Tapping Mode in an ambient atmosphere. Surface root mean square (RMS) roughnesses of 0.20 nm and 0.19 nm were determined from a standard analysis of AFM at a scan size of 200 nm $\times$ 200 nm, respectively.

All pentacene films were investigated using a Veeco Metrology Nanoscope LFM (lateral force microscopy)-3 atomic force microscope (Digital Instruments, Nanoscope IV) under atmospheric conditions. Transverse shear microscopy was performed using tips fabricated by Veeco Metrology, USA (triangular silicon nitride contact mode tips, model NP, force constant: 0.06–0.58 Nm^{-1}). The intra-island grain boundaries in a pentacene film were measured by determining the length of grain boundaries between two touching grains in one island; the edges of isolated islands were excluded, *i.e.*, we considered only intra-island grain boundaries. Then the intra-island grain-boundary density (ξ) was calculated by dividing the surface area by the length of inter-grain intra-island boundaries. The unit of the length of intra-island grain boundaries is nm, and μm^2 refers to the total surface area.

Results and discussion

Substrate analysis

As a typical dry cleaning method of surfaces prior to organic molecular film growth, UV/O_3 treatment is a well established method for cleaning surfaces and removing organic contamination.[22,29–32] After UV/O_3 treatment in an ambient atmosphere for 20 min, silicon oxide exhibits a hydrophilic character with a water contact angle of less than 5°, as determined by the sessile drop method.[22] Before treatment, this contact angle is 16° ± 2° for pristine silicon oxide cleaned by standard solvent processing.[21] Fig. 1 shows AFM images of pristine silicon oxide and UV/O_3-treated silicon oxide. The root mean square (RMS) roughness of the surfaces before and after UV/O_3 treatment was 0.20 nm and 0.19 nm, respectively. No significant morphological changes were observed. However, the phase images (Fig. 1(b) and (e)) of the substrates before and after UV/O_3 treatment present significant differences. This is further evidenced in Fig. 1(c) and (f) that show the effect of the AFM scanning history on phase images: for both samples, first an area of 200×200 nm^2 was scanned, followed by a second scan over 1×1 μm^2. On the UV/O_3-treated surface the phase image of the second scan clearly shows where the first scan was performed, while this is not the case for pristine silicon oxide. This points to a change in surface composition induced by the UV/O_3 treatment, which is unstable against removal by an AFM tip in the tapping mode.

Pristine and UV/O_3-treated silicon oxide surfaces were further investigated by XPS (see Fig. 2) in order to quantify possible changes in surface composition induced by the

UV/O_3 treatment. Before UV/O_3 exposure, carbon residue was detected, as can be seen from the C 1s core level spectrum in Fig. 2(a) [top curve, black line]. The surface-adsorbed C species on silicon oxide were mainly hydrocarbon contamination due to exposure to ambient air (binding energy of 285.8 eV),[33,34] 20 min UV/O_3 exposure led to a ∼30% decrease of the C 1s intensity. Differences in the intensity of the O 1s and Si 2p signals were barely noticeable [Fig. 2(b) and (c)]. Accordingly, we found for the surface stoichiometry (calculated from the measured C 1s, O 1s and Si 2p intensities weighted with the respective photoemission cross sections and analyser transmission at the different kinetic energies) of the two substrates that C decreases from 7.2% to 5.3%, O slightly increases from 61.8% to 63.3%, and Si is approximately constant (31.4% and 31.0%, respectively) after the UV/O_3 treatment. Most likely, hydrocarbon contamination, surface hydroxyls and/or bound oxygen radicals can act as additional pinning centres during pentacene layer growth (*vide infra*). Consequently, the additional pinning centres introduced on the silicon oxide surface by UV/O_3 treatment are not of morphological nature that could be detected by AFM, or significant surface composition changes in our experiments.

AFM and TSM characterisation of pentacene submonolayers

Transverse shear microscopy (TSM) is a variant of lateral force microscopy. It tracks the twisting of the cantilever due to the lateral forces acting perpendicular to the scan vector and can be used to visualise the relative orientation of grains in thin films with high contrast.[19,21,35–37] Fig. 3 shows transverse shear
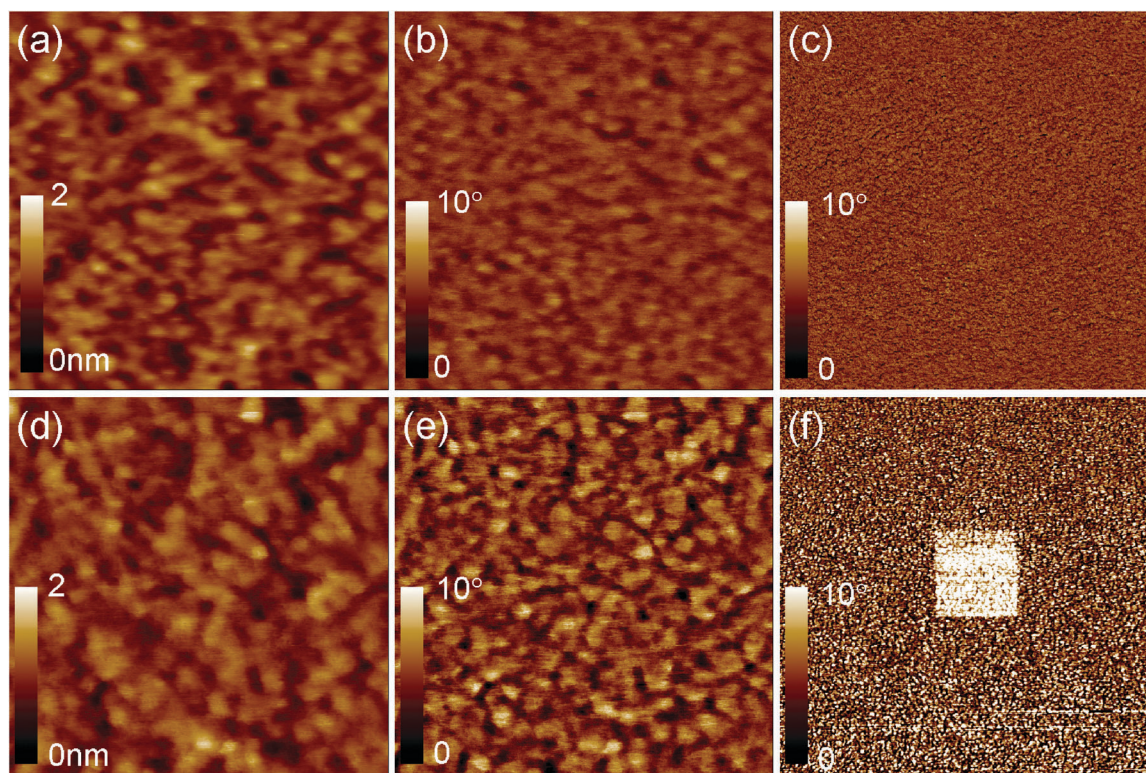
Fig. 1 Atomic force microscopy images acquired in tapping mode of pristine silicon oxide (a) 200 nm × 200 nm, height image, (b) 200 nm × 200 nm, phase image and (c) 1 μm × 1 μm, phase image; and of UV/O_3-treated silicon oxide (d) 200 nm × 200 nm, height image, (e) 200 nm × 200 nm phase image and (f) 1 μm × 1 μm, phase image.
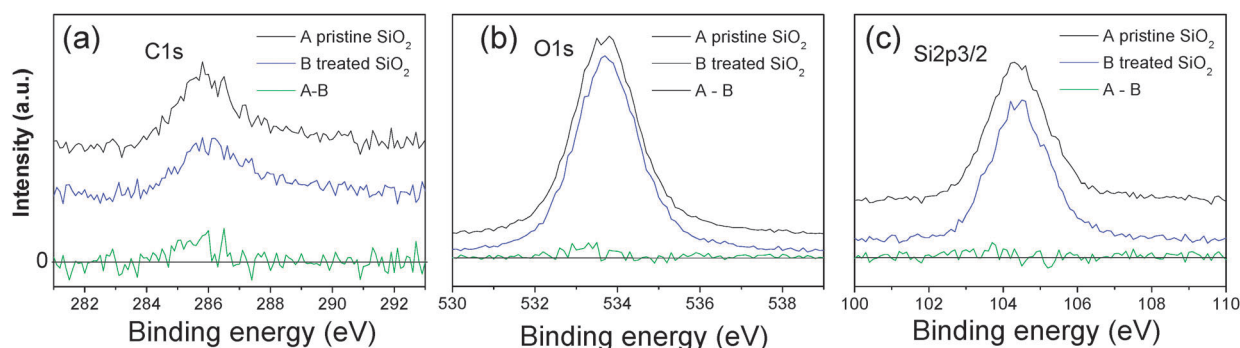
Fig. 2 C 1s (a), O 1s (b) and Si 2p3/2 (c) core level photoemission spectra of the pristine silicon oxide and UV/O$_3$-treated silicon oxide. Curves A, B, A–B are the spectrum of the pristine silicon oxide, the spectrum of the UV/O$_3$-treated silicon oxide, and the spectrum of the pristine silicon oxide minus the spectrum of the UV/O$_3$-treated silicon oxide.

microscopy images of pentacene films prepared by OMBD and SuMBD at various coverages in the sub-monolayer regime. OMBD films on pristine and UV/O$_3$-treated silicon oxides are shown in the first and second column from the left, respectively; the corresponding images of SuMBD samples are presented in the third and fourth column from the left. To derive the island density

for the different substrate preparations and pentacene deposition conditions, the molecular island count was averaged from five AFM images collected in different regions on each sample.

At a coverage (θ) of 0.17 ML equivalent, the island density of the OMBD film on pristine silicon oxide is 2.78 islands μm^{-2} [Fig. 3(a)], while on UV/O$_3$-treated silicon
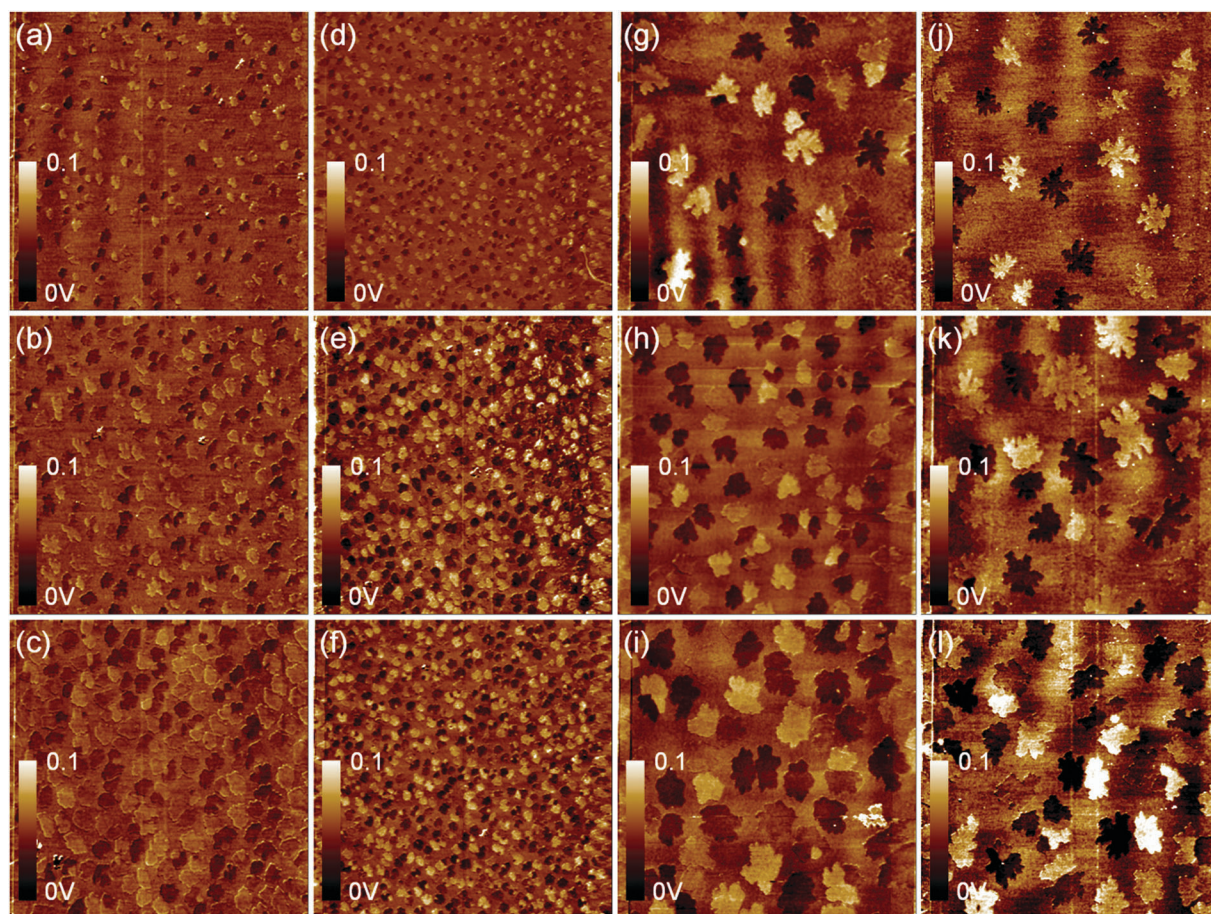
Fig. 3 Transverse shear microscopy images of pentacene sub-monolayers were acquired by *ex situ* contact mode atomic force microscopy scanning over an area of 10 μm × 10 μm. Images (a) (θ = 0.17 ML), (b) (θ = 0.32 ML) and (c) (θ = 0.53 ML) in the 1st column, and images (d) (θ = 0.26 ML), (e) (θ = 0.40 ML) and (f) (θ = 0.46 ML) in the 2nd column were obtained for samples grown by OMBD on pristine silicon oxide and on UV/O$_3$-treated silicon oxide, respectively. Images (g) (θ = 0.26 ML), (h) (θ = 0.36 ML) and (i) (θ = 0.53 ML) in the 3rd column, and images (j) (θ = 0.17 ML), (k) (θ = 0.36 ML) and (l) (θ = 0.42 ML) in the 4th column were obtained for samples grown by SuMBD on pristine silicon oxide and on UV/O$_3$-treated silicon oxide, respectively.

oxide we found 6.88 islands μm^{-2} at a similar coverage [Fig. 3(d)]. This reveals a striking difference in the nucleation density depending upon substrate preparation. For SuMBD pentacene films instead, the island density on pristine and on UV/O$_3$-treated is nearly the same, *i.e.*, 0.30 islands μm^{-2} at $\theta = 0.26$ ML [Fig. 3(g)] and 0.31 islands μm^{-2} at a similar coverage [Fig. 3(j)], respectively. The island densities of both SuMBD samples are more than one order of magnitude lower than those for pentacene films prepared by OMBD. Furthermore, the average size of the islands of films prepared by SuMBD is much larger than that of OMBD-films at the comparable coverage. Increasing the coverage to ~ 0.5 ML, the island density of the OMBD films remains almost constant [Fig. 3(c) and (f)]. Note that an unexpectedly high island density was observed in Fig. 3(h), which may be the result of an unstable molecular beam during deposition; therefore, values derived from this sample have larger error bars.

Intra-island grain-boundary density in pentacene sub-monolayers

The dependence of intra-island grain-boundary density (ξ) on θ of OMBD pentacene films on pristine and UV/O$_3$-treated silicon oxides is shown in Fig. 4 and suggests a linear increase of ξ with coverage for both types of substrates. Island coalescence does not contribute here because it sets in notably only for coverages higher than 0.5 ML.[21] A linear increase of ξ is stronger than expected for the case of a constant number of polycrystalline islands during island growth, where $\xi \approx \theta^{1/2}$ is expected. Extrapolating a linear fit of the data for OMBD-pentacene films yields a zero-value for ξ at $\theta \approx 0.05$ ML (pristine silicon oxide) and $\theta \approx 0.04$ ML (UV/O$_3$-treated silicon oxide), respectively. This suggests that new grain boundaries within single islands continuously form right from the beginning of the growth, long before island coalescence. The analogous data for SuMBD samples, also shown in Fig. 4, give a very different picture: the intra-island grain boundary density in SuMBD films on both substrates is much smaller than that in OMBD films with a similar coverage. Moreover, extrapolating the linear fit to $\xi = 0$ yields much higher values for the coverage at which grain boundaries start to form, *i.e.* ~ 0.20 ML for pristine and ~ 0.16 ML for UV/O$_3$-treated substrates.
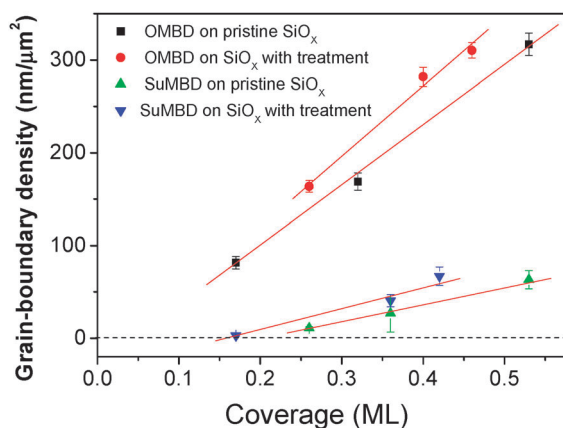
Fig. 4 The dependence of the intra-island grain-boundary density, ξ, on coverage, θ, in pentacene sub-monolayers deposited by OMBD and SuMBD on pristine and UV/O$_3$-treated silicon oxides.
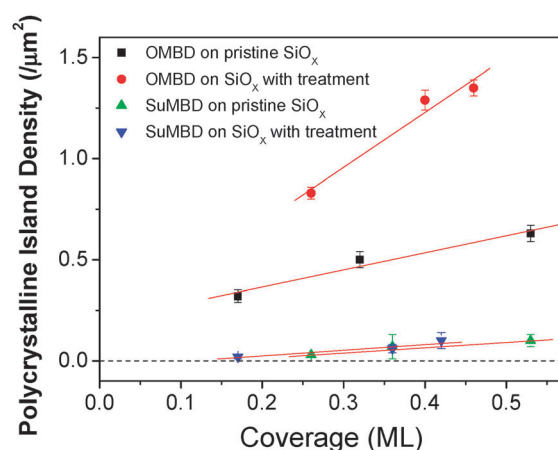
Fig. 5 The dependence of the polycrystalline island density on coverage, θ, in pentacene sub-monolayers by OMBD and SuMBD on pristine and UV/O$_3$-treated silicon oxides.

The density of polycrystalline islands in OMBD pentacene films on pristine and UV/O$_3$-treated silicon oxides (shown in Fig. 3) as a function of coverage is shown in Fig. 5. Clearly, the polycrystalline island density on UV/O$_3$-treated silicon oxide is much higher than that on pristine silicon oxide. The fact that the ratio of multi-grain islands is much higher for UV/O$_3$-treated substrates (where more additional pinning centres are present) suggests that polycrystalline island growth is the result of additional nucleation centres that introduce intra-island grain boundaries. The polycrystalline island density in SuMBD films on both types of substrates (Fig. 5) is also *circa* one order of magnitude lower than that in OMBD films with a similar coverage. When pentacene molecules from the gas phase land on the surface, the initial kinetic energy of pentacene is converted (partially) into kinetic energy parallel to the surface *via* a complex mechanism involving inelastic molecule–molecule and molecule–surface energy transfer processes. It is reasonable to assume, by extending consolidated growth models,[12] that molecules with higher kinetic energy diffuse over longer distances before being captured at already existing islands. Therefore, in SuMBD pentacene molecules diffuse much longer on pristine and UV/O$_3$-treated silicon oxides than in OMBD, and they have enough kinetic energy not to be trapped easily at the pinning centres. This largely masks the difference between pristine and UV/O$_3$-treated silicon oxides and results in similar island density and similar amount of polycrystalline islands. Furthermore, small bright protrusions can frequently be observed at the centre of separated islands in pentacene films by OMBD in the height images, and these protrusions are located at the intra-island grain boundaries in polycrystalline islands in TSM images (highlighted in Fig. 6 by white ovals), which proves that two or more stable pentacene nuclei can be formed simultaneously at surface pinning centres.[11] All these observations are consistent with the model (based on theoretical calculation) that polycrystalline growth may take place when nucleation centres introduce an increasing amount of disorder into dendrites and the growth is governed predominantly by diffusion limited aggregation.[38,39] In addition, the low intra-island grain boundary density in pentacene layers grown by SuMBD on substrates with various levels of extrinsic pinning sites implies a considerable decrease
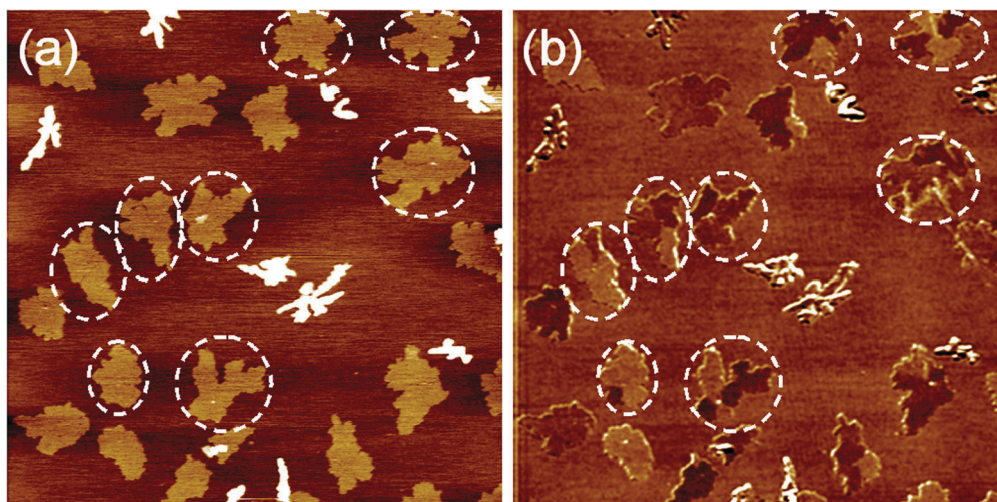
Fig. 6 Atomic force microscopy height image (a) and transverse shear microscopy image (b) of a pentacene film on silicon oxide with pinning centres [height scale in (a): 5 nm, scale in (b): 0.1 V]. Small bright protrusions at the centre of separated islands in pentacene films appear in the height images where intra-island grain boundaries in polycrystalline islands are seen in TSM images (white ovals highlighted in the figure), proving that two or more stable pentacene nuclei can be formed simultaneously at the surface pinning centre.

of possible charge carrier trapping sites in OTFTs fabricated with such films.[17–19]

Conclusion

In conclusion, a much higher pentacene island density and a higher density of polycrystalline islands were observed in pentacene films deposited by OMBD on UV/O$_3$-treated silicon oxide (with high pinning centre density) as compared to pristine silicon oxide. Pentacene films deposited by SuMBD showed instead a one order of magnitude lower polycrystalline island density on both types of substrates. Our results suggest that the growth of polycrystalline islands on amorphous silicon oxide is facilitated by surface pinning centres, which act as nucleation centres for multiple grain formation, forced into a single island. Furthermore, the lower intra-island grain boundary density in pentacene films fabricated by SuMBD implies a reduced number of charge carrier trapping sites directly at grain boundaries and should thus lead to increased charge carrier mobility, which is advantageous for their use in OTFTs.

Acknowledgements

References

1 T. W. Kelley, D. V. Muyres, P. F. Baude, T. P. Smith and T. D. Jones, *Mater. Res. Soc. Symp. Proc.*, 2003, **771**, L6.5.
2 S. Lee, B. Koo, J. Shin, E. Lee, H. Park and H. Kim, *Appl. Phys. Lett.*, 2006, **88**, 162109.
3 G. Horowitz, *Adv. Mater.*, 1998, **10**, 365–377.
4 H. Sirringhaus, N. Tessler and R. H. Friend, *Science*, 1998, **280**, 1741–1744.
5 C. D. Dimitrakopoulos and P. R. L. Malenfant, *Adv. Mater.*, 2002, **14**, 99–117.
6 J. G. Laquindanum, H. E. Katz, A. J. Lovinger and A. Dodabalapur, *Chem. Mater.*, 1996, **8**, 2542–2544.
7 Y.-Y. Lin, D. J. Gundlach, S. Nelson and T. N. Jackson, *IEEE Electron Device Lett.*, 1997, **18**, 606–608.
8 Z. Bao, A. Lovinger and A. Dodabalapur, *Adv. Mater.*, 1997, **9**, 42–44.
9 O. D. Jurchescu, M. Popinciuc, B. J. van Wees and T. T. M. Palstra, *Adv. Mater.*, 2007, **19**, 688–692.
10 F. J. M. Heringdorf, M. C. Reuter and R. M. Tromp, *Nature*, 2001, **412**, 517–520.
11 R. Ruiz, B. Nickel, N. Koch, L. C. Feldman, R. F. Haglund, A. Kahn, F. Family and G. Scoles, *Phys. Rev. Lett.*, 2003, **91**, 136102.
12 R. Ruiz, D. Choudhary, B. Nickel, T. Toccoli, K. C. Chang, A. C. Mayer, P. Clancy, J. M. Blakely, R. L. Headrick, S. Iannotta and G. G. Malliaras, *Chem. Mater.*, 2004, **16**, 4497–4508.
13 B. Nickel, R. Barabash, R. Ruiz, N. Koch, A. Kahn, L. C. Feldman, R. F. Haglund and G. Scoles, *Physical Review B: Condens. Matter*, 2004, **70**, 125401.
14 Y. Wu, T. Toccoli, N. Koch, E. Iacob, A. Pallaoro, P. Rudolf and S. Iannotta, *Phys. Rev. Lett.*, 2007, **98**, 076601.
15 V. Kalihari, D. J. Ellison, G. Haugstad and C. D. Frisbie, *Adv. Mater.*, 2009, **21**, 3092–3098.
16 R. Ruiz, A. Papadimitratos, A. C. Mayer and G. G. Malliaras, *Adv. Mater.*, 2005, **17**, 1795–1798.
17 J. H. Kang, D. da Silva, J. L. Bredas and X. Y. Zhu, *Appl. Phys. Lett.*, 2005, **86**, 152115.
18 Y. Jung, R. J. Kline, D. A. Fischer, E. K. Lin, M. Heeney, I. McCulloch and D. M. DeLongchamp, *Adv. Funct. Mater.*, 2008, **18**, 742–750.
19 K. Puntambekar, J. P. Dong, G. Haugstad and C. D. Frisbie, *Adv. Funct. Mater.*, 2006, **16**, 879–884.
20 J. T. Sadowski, G. Sazaki, S. Nishikata, A. Al-Mahboob, Y. Fujikawa, K. Nakajima, R. M. Tromp and T. Sakurai, *Phys. Rev. Lett.*, 2007, **98**, 046104.
21 J. Zhang, J. P. Rabe and N. Koch, *Adv. Mater.*, 2008, **20**, 3254–3257.
22 A. W. Neumann and R. J. Good, in *Surface and Colloid Science*, ed. R. J. Good and R. R. Stromberg, Plenum, New York, 1979, vol. 11.
23 S. Wo, B. Wang, H. Zhou, Y. Wang, J. Bessette, R. L. Headrick, A. C. Mayer, G. G. Malliaras and A. Kazimirov, *J. Appl. Phys.*, 2006, **100**, 093504.

24 S. Iannotta and T. Toccoli, *J. Polym. Sci., Part B: Polym. Phys.*, 2003, **41**, 2501–2521.

25 S. Iannotta, T. Toccoli, F. Biasioli, A. Boschetti and M. Ferrari, *Appl. Phys. Lett.*, 2000, **76**, 1845–1847.

26 L. Aversa, R. Verucchi, G. Ciullo, L. Ferrari, P. Moras, M. Pedio, A. Pesci and S. Iannotta, *Appl. Surf. Sci.*, 2001, **184**, 350–355.

27 A. Podesta, T. Toccoli, P. Milani, A. Boschetti and S. Innotta, *Surf. Sci.*, 2000, **464**, L673–L680.

28 Y. Wu, T. Toccoli, J. Zhang, N. Koch, E. Iacob, A. Pallaoro, S. Iannotta and P. Rudolf, *Appl. Phys. A: Mater. Sci. Process.*, 2009, **95**, 21–27.

29 M. Zimmer, M. Burgmair, K. Scharnagl, A. Karthigeyan, T. Doll and I. Eisele, *Sens. Actuators, B*, 2001, **80**, 174–178.

30 J. G. Xue and S. R. Forrest, *J. Appl. Phys.*, 2004, **95**, 1869–1877.

31 Y. Suzue, T. Manaka and M. Iwamoto, *Jpn. J. Appl. Phys.*, 2005, **44**, 561–565.

32 D. Guo, S. Entani, S. Ikeda and K. Saiki, *Chem. Phys. Lett.*, 2006, **429**, 124–128.

33 D. S. Campbell, H. J. Leary, J. S. Slattery, R. J. Sargent, *ESCA Surface Analysis of Plasma Exposed Silicon Nitride and Photoresist Polymer*, IBM General Technology Division (ed.), Essex Junction, VT 05452, 328.

34 P. Bertrand, V. B. Wiertz, *Identification of the N-containing functionalities introduced at the surface of ammonia plasma treated carbon fibres by combined TOF SIMS and XPS*, Unité de Physico-Chimie et de Physique des Matériaux, Université Catholique de Louvain (editor), Louvain, Belgium.

35 J. A. Last and M. D. Ward, *Adv. Mater.*, 1996, **8**, 730–733.

36 M. Campione and E. Fumagalli, *Phys. Rev. Lett.*, 2010, **105**, 166103.

37 V. Kalihari, G. Haugstad and C. D. Frisbie, *Phys. Rev. Lett.*, 2010, **104**, 086102.

38 L. Granasy, T. Pusztai, J. A. Warren, J. F. Douglas, T. Boerzsoenyi and V. Ferreiro, *Nat. Mater.*, 2003, **2**, 92–96.

39 K. Taguchi, H. Miyaji, K. Izumi, A. Hoshino, Y. Miyamoto and R. Kokawa, *Polymer*, 2001, **42**, 7443–7447.